

Magnetic-field-induced type-I \rightarrow type-II transition in a semimagnetic CdTe/Cd_{0.93}Mn_{0.07}Te superlattice

E. Deleporte, J. M. Berroir, G. Bastard, and C. Delalande

Laboratoire de Physique de la Matière Condensée de l'Ecole Normale Supérieure, 24 rue Lhomond, 75005 Paris, France

J. M. Hong and L. L. Chang

IBM Research Division, Thomas J. Watson Research Center, P. O. Box 218, Yorktown Heights, New York 10598

(Received 7 May 1990)

Magnetophotoluminescence- and photoluminescence-excitation-spectroscopy experiments are performed up to 5 T at 1.7 K in a $\langle 111 \rangle$ -grown CdTe/Cd_{0.93}Mn_{0.07}Te superlattice. The results are compared with calculations of the level energies and of the exciton binding energies, that include field-induced negative offsets. A type-I \rightarrow type-II transition is evidenced near 2 T and a value of 15%–20% of the band-gap energy difference is deduced for the valence-band offset.

The recent growth by molecular-beam epitaxy of diluted magnetic-semiconductor compounds has made possible the study of optical¹ or magnetic² properties of superlattices such as CdTe/Cd_{1-x}Mn_xTe. One of the key differences with the GaAs/Ga_{1-x}Al_xAs system is the large magnetic-field variation of the Ce-Mn-Te band gap, and thus of the CdTe/Cd_{1-x}Mn_xTe conduction-band and valence-band offsets. These effects arise from the exchange interaction between the magnetic ions and the carriers.^{3,4} Associated with the possible small value of the valence-band offset ΔE_v ,¹ a magnetic tuning of ΔE_v might lead to a type-I \rightarrow type-II transition at a moderate magnetic field in the case of low Mn concentration in the barrier. This transition was first observed very recently in another system: ZnSe/Zn_{1-x}Fe_xSe,⁵ and may be due to the very low ΔE_v and the strain state found in this case. The formation and modification of superlattice minibands by an external magnetic field through the exchange interaction of itinerant carriers with localized ions was first predicted by von Ortenberg.⁶

We report here evidence of a type-I \rightarrow type-II magnetic-field-induced transition for one-spin component of the holes in a $\langle 111 \rangle$ -grown 86-Å–86-Å CdTe/Cd_{0.93}Mn_{0.07}Te 25-period superlattice. This superlattice is grown on top of a $\langle 100 \rangle$ GaAs substrate after a 1500-Å-thick CdTe buffer layer. This conclusion is supported by three observations: a well marked bump in the field dependence of the fundamental $\sigma^+ e_1$ -hh₁ excitonic transition; a break in the variation of the photoluminescence efficiency, and a strong redshift of the onset of the photoluminescence-excitation spectrum of a line associated with impurities located in the barrier. These three features take place around the same field value ≈ 2 T. We point out that the variation of the binding energy of the exciton in this low- ΔE_v (and even negative- ΔE_v) system is essential for the comparison with experiment.

Figure 1(a) shows the luminescence spectrum (dashed line) of the superlattice at zero-magnetic field. Two lines: PL and PL' are observed which peak at ≈ 1622 and 1585 meV, respectively. The photoluminescence-excitation spectrum of the PL line [solid line in Fig. 1(a)] shows a well marked A peak at ≈ 1624 meV flanked by a weak should-

der around 1635 meV. The onset of the excitation spectrum of the PL' line [dashed-dotted line in Fig. 1(a)] is located near 1635 meV (line B), the remainder of the spectrum is essentially the same as that of the PL line. Complementary reflectivity and piezomodulation experiments, whose details will be published elsewhere,⁷ have shown that the in-plane stress in the system for CdTe is $\epsilon_{\text{CdTe}} \approx -0.2\%$, which leads to a heavy-hole-light-hole splitting of 12 meV for the CdTe buffer, the light-hole lying at the higher energy. For an elastic accommodation of

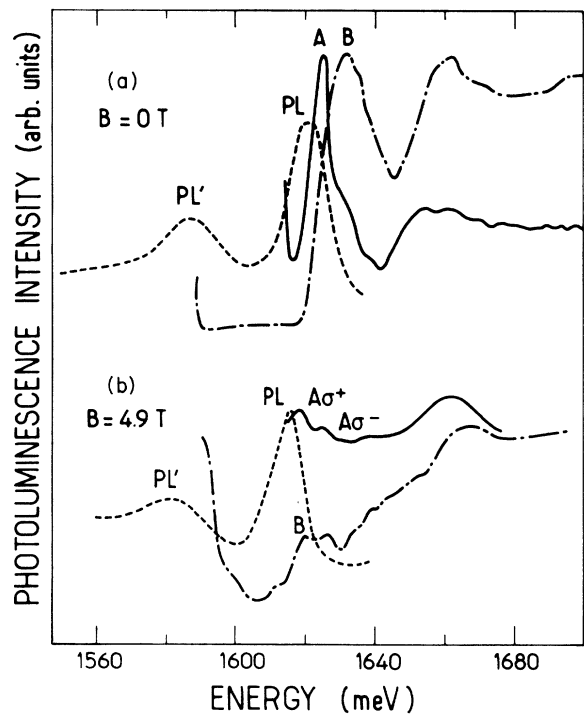


FIG. 1. Photoluminescence spectrum (dashed curve), photoluminescence-excitation spectra of the PL line (solid curve) and of the PL' line (dashed-dotted curve) for a 86-Å–86-Å $\langle 111 \rangle$ -grown CdTe/Cd_{0.93}Mn_{0.07}Te 25-period superlattice under (a) zero-magnetic field and (b) a magnetic field $B = 4.9$ T.

the Cd-Mn-Te barrier, we find a stress value $\epsilon_{\text{Cd-Mn-Te}} \approx -0.09\%$ for the barrier.⁸ A calculation of the energy levels in the framework of the three-band envelope-function approximation⁹ has been performed using the following parameters: $m_e = 0.096m_0$, $m_h = 0.6m_0$, the spin-orbit splitting $\Delta = 1$ eV, $E_g(\text{Cd}_{1-x}\text{Mn}_x\text{Te}) = 1610 + 1564x$ (meV) and a variable valence-band offset. This calculation complemented by that of the exciton binding energy (see below) shows that line *A* is associated with the excitonic hh_1-e_1 $1s$ transition energy while line *B* could be related to the excitonic e_1-lh_1 transition. Note that the comparison between theory and experiment does not provide a precise measurement of ΔE_v , as usually found in superlattice systems. The PL line corresponds to weakly bound excitons whereas the low-energy PL' line should be associated with acceptorlike defects (as the sample is *p* type) of the Cd-Mn-Te barrier: the onset of its excitation spectrum corresponds to the onset of rather delocalized light-hole states (the lh_1 miniband width is 7 meV for an offset $\Delta E_v \sim 15$ meV). This promotes a trapping of photo-created light holes by the defects of the barriers, in opposition with heavy holes whose wave function hardly penetrates the barrier, at least at zero-magnetic field and large enough ΔE_v .

The sample was inserted in a superconducting magnet up to 5 T at a controlled temperature at 1.7 K. Laser-

ingoing and photoluminescence-outgoing lights were collected by a multi-fiber-optic guide. Figure 1(b) shows the photoluminescence- and photoluminescence-excitation spectra obtained at $B = 4.9$ T. The PL and PL' lines exhibit a redshift whereas the $X_{e_1-hh_1}$ excitonic *A* line is divided into two A_{σ^+} and A_{σ^-} lines in the standard way.⁴ The onset *B* of the excitation spectrum of the PL' line is strongly redshifted and appears almost at the same energy as the A_{σ^+} line at large magnetic field, in striking contrast with the zero-field situation. The experimental magnetic-field dependence of the peak energies are plotted in Fig. 2(a) by crosses (PL), and open circles (*B*). A bump in the redshift is observed, especially in the PL variation near 2 T. In the same field range, the *B* onset energy displays a precipitous drop. Through it is not presented here for the sake of simplicity, the A_{σ^-} line follows the usual variation towards high energy with the magnetic field and without any accident in the observed shift. Finally, the measurement of the relative radiative yield ρ of the PL line, reproduced in Fig. 2(b), shows that ρ decreases by a factor of 2 up to 2–2.5 T and remains almost constant at larger magnetic fields.

The results of the calculation of the quantum-well exciton binding energy, which is necessary for a comparison between theory and experiment, are plotted in Fig. 3 as a function of the unknown ΔE_v offset. The details of the calculation, whose assumptions are close to those of Chang *et al.*,¹⁰ will be published elsewhere.⁷ Briefly, a variational approach, in the diagonal approximation of the excitonic Hamiltonian,⁹ has been undertaken under the assumption that, due to the large conduction-band offset, the longitudinal electron motion is forced by the

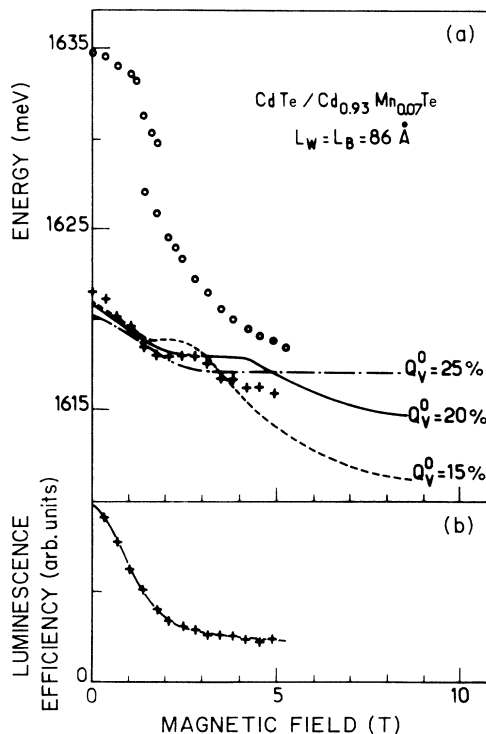


FIG. 2. Upper panel: Experimental magnetic-field variation of (crosses) the PL-line energy, and (circles) of the onset *B* of the excitation spectrum of the PL' line. The curves correspond to the theoretical calculations of the $X_{e_1-hh_1}(\sigma^+)$ transition as explained in the text at three values of the relative strain-free valence-band offset $Q_v^0 = \Delta E_v^0 / \Delta E_g^0 = 15\%$, 20%, and 25%. Lower panel: Experimental magnetic-field variation of the luminescence efficiency of the PL line.

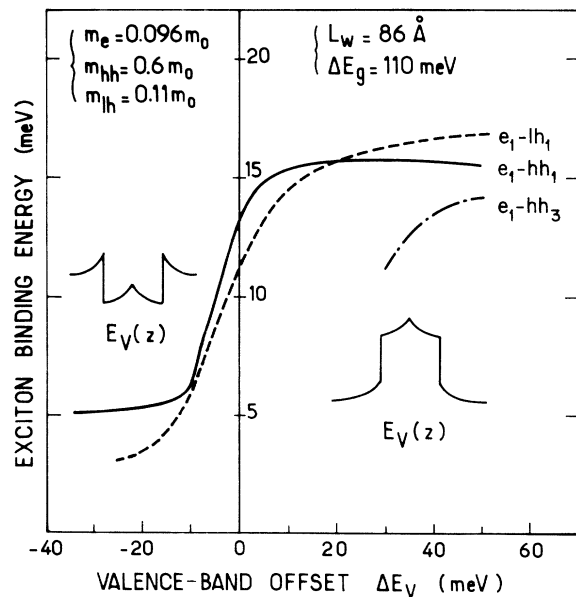


FIG. 3. Calculated binding energy of the e_1-hh_1 $1s$ exciton vs the valence-band offset in the investigated structure. The insets show the potential seen by the hole resulting from the Coulombic interaction with the electron in the growth direction at negative (left-hand side) and positive (right-hand side) ΔE_v . A positive ΔE_v means a confined motion in the CdTe layer (type-I case).

quantum-well potential (the e_1 state), while the longitudinal hole motion takes place in an effective one-dimensional potential which is the sum of the superlattice potential and of the Coulombic potential averaged over the probability densities of the electron and reduced in-plane motion. The potential seen by the hole is shown in Fig. 3 both for a positive (right-hand side) and negative (left-hand side) ΔE_v . Taking a $1s$ -like exponential wave function for the in-plane exciton motion, the energy difference between the transition energies with and without Coulombic interaction provides the calculation of the exciton binding energy E_x both for positive and negative offsets. A rapid decrease of E_x from ~ 15 meV down to ~ 5 meV is found in an offset range of 10 meV around the vanishing offset.

The large exchange mechanisms in the Cd-Mn-Te layer modify the actual offsets $\Delta E_c(B, m_J)$ and $\Delta E_v(B, m_J)$ in the presence of the magnetic field. We took the parameters reported in Ref. 3 in the bulk for the calculation of conduction, light-hole, and heavy-hole giant Zeeman splittings. For each value of B , i.e., for each value of $\Delta E_v(B, m_J)$ and $\Delta E_c(B, m_J)$, the calculations of the band-to-band transition and of the exciton binding energy have been performed. The diamagnetic shift of the exciton was neglected with respect to the giant Zeeman splitting. In our calculation, we took into account the stress. The strained value ΔE of the zero-magnetic offsets are deduced from the strain free ΔE_v^0 by $\Delta E_v^{\text{hh}} = \Delta E_v^0 + 2.2$ meV, $\Delta E_c = \Delta E_c^0 - 2.6$ meV for heavy holes and electrons, respectively.⁷

The theoretical variation of the $X_{e_1\text{-hh}_1}(\sigma^+)$ transition energies are plotted in Fig. 2 (curves) for three values of ΔE_v^0 : $0.15\Delta E_c^0$ (dashed line), $0.2\Delta E_c^0$ (solid line), and $0.25\Delta E_c^0$ (dashed-dotted line) with $\Delta E_c^0 = 110$ meV. The presence of a bump in the field variation of the fundamental transition is striking and it resembles that found experimentally. This bump occurs near the type-I → type-II transition and is related to the fast decrease of the exciton binding energy. This decrease is faster than the decrease of the band-to-band energy and therefore induces a small increase or at least a plateau, in the variation of the transition energy versus the magnetic field. The type-I → type-II transition occurs theoretically at $B = 1.2, 1.9,$ and 2.5 T for $\Delta E_v^0/\Delta E_c^0 = 0.15, 0.2,$ and 0.25 , respectively.

The two other experimental findings corroborate this strong indication of a magnetic-field-induced type-I → type-II transition. With decreasing ΔE_v , the heavy-hole wave function penetrates more and more in the Cd-Mn-Te barrier. Thus the overlap with possible defects of the ternary alloy is larger, leading to an increase of possible nonradiative channel efficiency (and also a decrease of the radiative rate). When the offset becomes negative enough, the Coulombic interaction keeps the hole near the interface, leading to a constant binding energy of the exciton (Fig. 3) and to a constant interaction with the defects of the barrier. The variation of the radiative efficiency induced by the variation of the magnetic field becomes weaker, as found experimentally.

Finally, the strong redshift in the B onset of the excitation spectrum of the PL' line is easily explained if one supposes that this line is related to trapping of holes localized

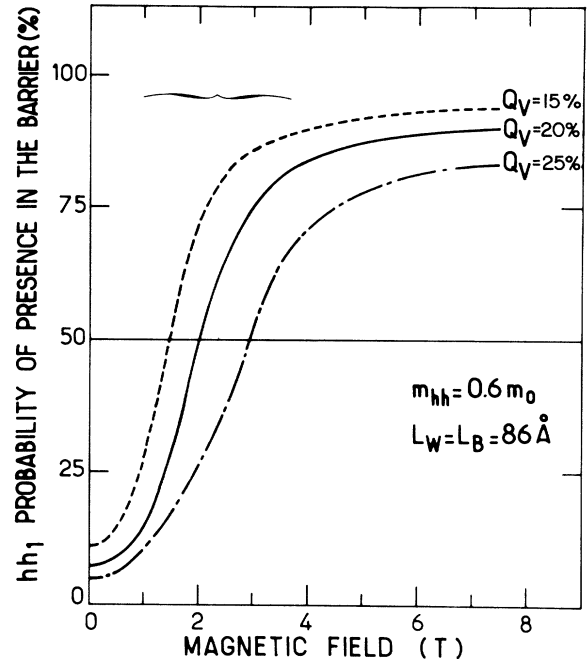


FIG. 4. Magnetic-field dependence of the integrated probability of finding the hole in the $\text{Cd}_{0.93}\text{Mn}_{0.07}\text{Te}$ layers while in the hh_1 state. The type-I → type-II transition (brace) occurs when this probability is equal to 50%.

in the Cd-Mn-Te barrier. At low field, the lowest-lying hole state delocalized in the barrier is the light-hole state. We found theoretically a probability of presence in the barrier for the lh_1 (hh_1) in the range of 35% (10%) at $B = 0$. Above the type-I → type-II transition, the heavy-hole state becomes localized in the barrier (50% at vanishing offset) and the B line corresponds to the $X_{e_1\text{-hh}_1}(\sigma^+)$ line. We show in Fig. 4, the magnetic-field dependence of the integrated probability of finding the hole in the $\text{Cd}_{0.93}\text{Mn}_{0.07}\text{Te}$ layers while in the hh_1 state to illustrate the progressive evolution from a type-I to a type-II configuration.

In conclusion, we have obtained strong indications of a magnetic-field-induced type-I → type-II transition in a semimagnetic CdTe/ $\text{Cd}_{0.93}\text{Mn}_{0.07}\text{Te}$ superlattice. This transition is induced by the giant Zeeman splitting of the heavy-hole Cd-Mn-Te edge. The calculations show that the rapid decrease of the exciton binding energy is an essential feature in the understanding of this transition. This transition occurs for a magnetic field in around 2 T, which is theoretically sensitive to the zero-field and strain-free valence-band offset ΔE_v^0 . From our measurements, we obtain a value of the relative strain-free valence-band offset $Q_v^0 = \Delta E_v^0/\Delta E_c^0$ near 15%–20%, a value which is slightly larger than those reported in other samples.¹

We would like to thank B. Gil for his participation to the determination of the strain in the structure⁷ and M. Voos for his constant interest for this work. This study has been partly supported by an U.S. Army Research Office contract. One of us (G.B.) is supported by the Centre National de la Recherche Scientifique.

- ¹A. V. Nurmikko, R. L. Gunshor, and L. A. Kolodziejzski, *IEEE Quantum Electron.* **QE-22**, 1785 (1986).
- ²D. D. Awschalom, J. Warnock, J. M. Hong, L. L. Chang, M. B. Ketchen, and W. J. Gallagher, *Phys. Rev. Lett.* **62**, 199 (1989).
- ³J. A. Gaj, R. Planel, and G. Fishmann, *Solid State Commun.* **29**, 435 (1979).
- ⁴J. Warnock, A. Petrou, R. N. Bicknell, N. C. Giles-Taylor, O. K. Blanks, and J. F. Schetznina, *Phys. Rev. B* **32**, 816 (1985).
- ⁵X. Liu, A. Petrou, J. Warnock, B. T. Jonker, G. A. Prinz, and J. J. Kretz, *Phys. Rev. Lett.* **63**, 2280 (1989).
- ⁶M. von Ortenberg, *Phys. Rev. Lett.* **49**, 1041 (1982).
- ⁷E. Deleporte, B. Gil, J. M. Berroir, C. Delalande, G. Bastard, M. Hong, and L. L. Chang (unpublished).
- ⁸For the values of the parameters, see *Diluted Magnetic Semiconductors*, *Semiconductors and Semimetals*, Vol. 25, edited by J. K. Furdyna and J. Kossut (Academic, New York, 1988).
- ⁹G. Bastard, in *Wave Mechanics Applied to Semiconductor Heterostructures* (Les Editions de Physique, Les Ulis, France, 1989).
- ¹⁰S. K. Chang, A. V. Nurmiko, J. W. Liu, L. A. Kolodziejzski, and R. L. Gunshor, *Phys. Rev. B* **37**, 1191 (1988).